Electron-Cloud Build-up in the FNAL Main Injector*

M. A. Furman,† Center for Beam Physics, LBNL, Berkeley, CA 94720-8211, USA

Abstract

We present a summary on ongoing simulation results for the electron-cloud buildup in the context of the proposed FNAL Main Injector (MI) intensity upgrade [1] in a field-free region at the location of the RFA electron detector [2]. By combining our simulated results for the electron flux at the vacuum chamber wall with the corresponding measurements obtained with the RFA we infer that the peak secondary electron yield (SEY) $\delta_{\max}$ is $\gtrsim 1.4$, and the average electron density is $n_e \gtrsim 10^{10}$ m^{-3} at transition energy for the specific fill pattern and beam intensities defined below. The sensitivity of our results to several variables remains to be explored in order to reach more definitive results. Effects from the electron cloud on the beam are being investigated separately [3].

INTRODUCTION

An upgrade to the MI at FNAL is being considered that would increase the bunch intensity to $N_b \sim 3 \times 10^{11}$ in order to generate intense beams for the neutrino program [1]. While such high intensities will require significant hardware upgrades, the technique of slip-stacking routinely allows, at present, bunch intensities $N_b \gtrsim 1 \times 10^{11}$. During 2006 an RFA-type electron detector was installed in a field-free section of the MI, which shows a clear electron cloud signal close to transition energy at such beam intensities [2].

In response to these developments, we have been examining, by means of simulations with the build-up code POSINST [4–7], the magnitude of the electron-cloud effect and the potential risks thereof at higher values of N_b [8–12]. The present RFA measurements allow a first calibration of our results and therefore a prediction for the electron cloud density expected at higher intensity. This article summarizes Ref. [11] and slightly corrects and clarifies its conclusions.

SIMULATED CONDITIONS

The MI beam ramps from injection at a kinetic energy $K = 8$ GeV to extraction at $K = 120$ GeV in ~ 0.5 s, corresponding to $\sim 45,000$ turns, crossing transition at $K \simeq 20$ GeV. Ideally, we would simulate the entire ramp, but this is wholly beyond our present-day computer capabilities. We have therefore simulated only 3 values of K, namely $K = 8$, 20 and 30 GeV, and only for one full revolution in each case (revolution period $T_0 = 11.1$ μs). For each value of K, we assume two representative values for the RMS bunch length. We assume a bunch fill pattern made up of 6 batches, each having a train of 82 bunches followed by 4 empty buckets. The first batch is a double-intensity batch, with $N_b = 10.3 \times 10^{10}$, while the bunches in the remaining batches have a more standard intensity $N_b = 5.7 \times 10^{10}$. There is a 76-bucket-long gap after the last bunch of the 6th train for a total of 588 buckets. The bunch spacing in time is $t_b = 18.8$ ns.

We simulate the electron cloud build-up only in the field-free section where the RFA electron detector is installed. At this location the chamber is cylindrical of radius $R = 7.3$ cm and the beta functions are $(\beta_x, \beta_y) = (20, 30)$ m. We assume a normalized 95% transverse emittance $\epsilon_{n,95\%} = 15\pi$ mm-mrad for all bunches for all cases we investigate here. The energy spread is small enough that the dispersion contributes negligibly to the transverse beam size. We further assume the stainless steel SEY model described in [5, 6], with the additional practical assumption that the SEY at 0 energy, $\delta(0)$, is proportional to $\delta_{\max}$. This latter is the primary variable exercised in this set of simulations: we allow it to range in $1.3 \leq \delta_{\max} \leq 1.7$. However, we keep fixed $E_{\max}$, the incident electron energy at which the SEY peaks, at 293 eV. Table 1 shows the RMS transverse beam sizes and other beam parameters. Other simulation details and variables such as grid size and number of macroparticles are discussed in [11].

RESULTS

Fig. 1 represents one example of the time development of the average electron cloud density n_e during one machine revolution assuming $\delta_{\max} = 1.3$. In this case n_e grows exponentially during the first batch owing to the high value of N_b, and then decays to a negligible level during the passage of the rest of the beam. For higher values of $\delta_{\max}$, n_e reaches or exceeds the beam neutralization level, as discussed below.

Figs. 2 show the one-turn-average incident electron flux J_e at the wall of the chamber vs. $\delta_{\max}$ for the 6 cases considered, as labeled. Figs. 3 show n_e for the same conditions. Several other quantities related to the electron cloud, such as average electron-wall impact energy and local density, are discussed in [11].

DISCUSSION

An approximate proportionality between J_e and n_e is evident in our simulated data, not just for the one-turn av-

* Work supported by the FNAL HINS R&D Effort and by the US DOE under contract DE-AC02-05CH11231. Proc. ECLOUD07 Workshop, Daegu (S. Korea, April 9-12, 2007), http://chep.knu.ac.kr/ecloud07

† mafurman@lbl.gov

Table 1: Assumed beam parameters.

Beam kinetic energy	K [GeV]	8	20	30
Beam relativistic factor	γ_b	9.486	22.32	32.97
95% bunch duration	T_b [ns]	8 or 6	1 or 0.75	1.8 or 1.5
RMS bunch length	σ_z [m]	0.596 or 0.447	0.0749 or 0.0562	0.135 or 0.112
Hor. RMS bunch size	σ_x [mm]	2.29	1.50	1.23
Vert. RMS bunch size	σ_y [mm]	2.81	1.83	1.51

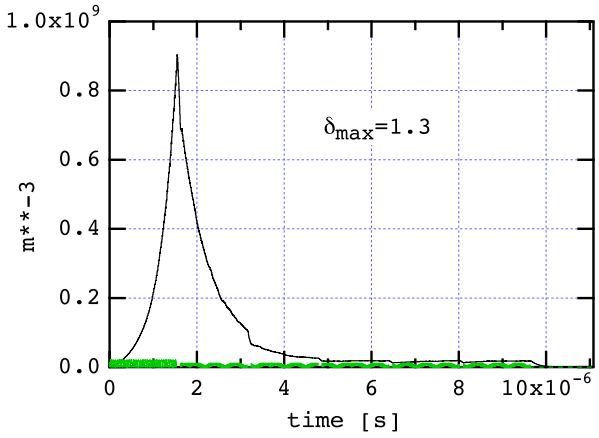

Figure 1: Simulated electron density n_e as a function of time for one revolution for $\delta_{\max} = 1.3$. The green vertical lines represent the beam signal (arbitrary units).

erages in Figs. 2-3 but also for the time-dependent quantities, for all cases we have simulated. This proportionality is a simple consequence of the assumption that all electrons contained in the chamber at any given time will strike the wall within a time interval $= t_b$.[1] For a round chamber, this assumption readily yields

$$J_e = kn_e\,, \qquad k = \frac{eR}{2t_b} \tag{1}$$

Our simulation conditions yield $k = 0.3 \times 10^{-12}$ A–m, which is satisfied by all our simulations for the MI at the RFA location within a factor of 2 or better. Presumably, this agreement becomes less good for smaller t_b and/or smaller N_b.

A change in the qualitative dependence of n_e (or J_e) on $\delta_{\max}$ is seen in Figs. 2-3 at $\delta_{\max} \simeq 1.4 - 1.6$: the dependence is exponential below this threshold, and linear above it. This change is probably due to the transition from a non-space-charge dominated electron cloud density to a space-charge dominated regime.

The simulations near transition energy, $K = 20$ GeV, show significantly higher values of n_e and J_e than at injection energy, in qualitative agreement with observations. The mechanism for the more intense effect is a

[1] I am indebted to R. Zwaska for this argument.

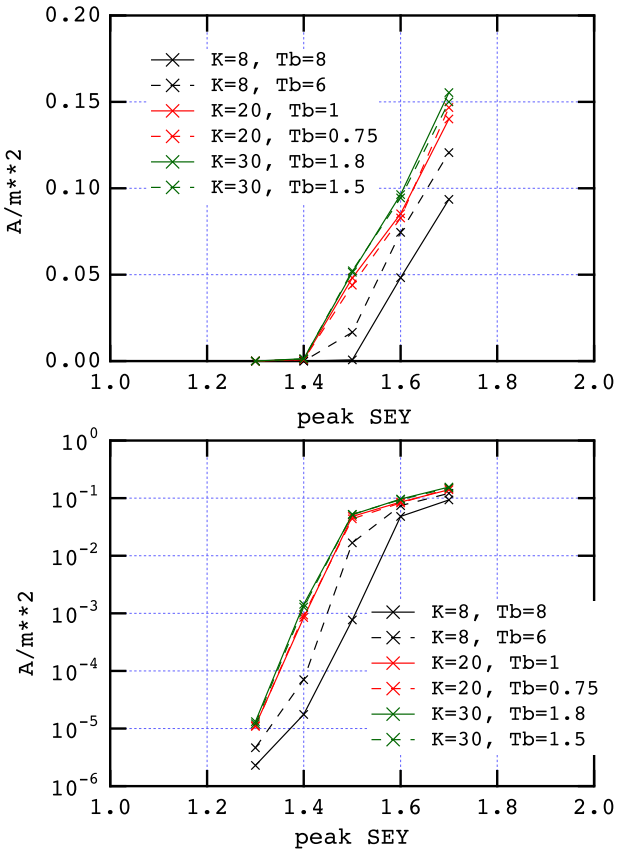

Figure 2: Simulated electron flux at the walls of the chamber vs. $\delta_{\max}$ for the various cases simulated. Top: linear scale; bottom: logarithmic scale (same data).

stronger kick by the beam on the electrons owing to the shorter bunch length. This stronger kick implies an average electron-wall collision energy that approaches or exceeds $E_{\max}$ [12], implying, in turn, a higher effective SEY.

Although the overall electron-cloud density is seen to exceed the beam neutralization level by up to $\sim 30\%$ in Figs. 3 at $\delta_{\max} = 1.7$, the electron-cloud density within the 1-σ beam ellipse (not shown here) is only a few percent of the local beam neutralization level, $N_b/(\pi\sigma_x\sigma_y s_b)$, which is in the range $(0.5 - 1.7) \times 10^{15}$ m^{-3} for the cases considered (s_b is here the bunch spacing in units of length).

The electron current measured by the RFA detector [14] is $\sim 0.1 - 0.3$ μA near transition energy, corresponding to

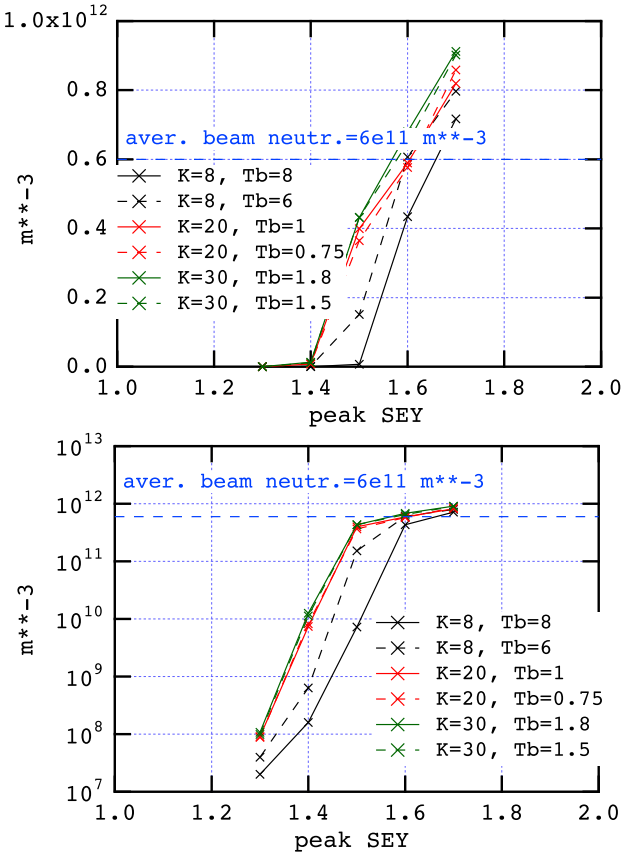

Figure 3: Simulated electron density vs. $\delta_{\max}$ for the various cases simulated. Top: linear scale; bottom: logarithmic scale (same data).

a flux $J_e \sim 0.7 - 2$ mA/m^2. Comparing this value with Figs. 2 implies $\delta_{\max} \gtrsim 1.4$, and $n_e \gtrsim 10^{10}$ m^{-3}, with a significantly lower density at $K = 8$ GeV. This value of $\delta_{\max}$ is in disagreement with the value obtained from a direct bench measurement of a MI vacuum chamber sample at SLAC, namely $\delta_{\max} \simeq 2$ [15]. It appears, however, that the sample in question was exposed to air before its SEY was measured; this could explain the much larger value than what we infer from our simulations.

Our simulations may be sensitive to other model variables, which we have not yet explored, that may change details of our conclusions. Such variables include:

- The precise value of $\delta(0)$.
- The detailed composition of the secondary emission energy spectrum, particularly the fraction of rediffused electrons.
- The precise value of $E_{\max}$.

More detailed discussions are presented in [11].

ACKNOWLEDGMENTS

I am indebted to R. Zwaska for discussions and guidance on this work, and for the arguments leading to Eq. (1). I am grateful to NERSC for supercomputer support.

REFERENCES

[1] Proton Driver Study. II. (Part 1, ch. 13), FERMILAB-TM-2169 (G. W. Foster, W. Chou and E. Malamud, eds.), May 2002.

[2] R. Zwaska, these proceedings.

[3] K. Sonnad, these proceedings.

[4] M. A. Furman and G. R. Lambertson, "The electron-cloud instability in the arcs of the PEP-II positron ring," LBNL-41123/CBP Note-246, PEP-II AP Note AP 97.27 (Nov. 25, 1997). Proc. *Intl. Workshop on Multibunch Instabilities in Future Electron and Positron Accelerators "MBI-97"* (KEK, 15-18 July 1997; Y. H. Chin, ed.), KEK Proceedings **97-17**, Dec. 1997, p. 170.

[5] M. A. Furman and M. T. F. Pivi, "Probabilistic model for the simulation of secondary electron emission," LBNL-49771/CBP Note-415 (Nov. 6, 2002). PRST-AB **5** 124404 (2003), http://prst-ab.aps.org/pdf/PRSTAB/v5/i12/e124404.

[6] M. A. Furman and M. T. F. Pivi, "Simulation of secondary electron emission based on a phenomenological probabilistic model," LBNL-52807/SLAC-PUB-9912 (June 2, 2003).

[7] M. A. Furman, "The electron-cloud effect in the arcs of the LHC," LBNL-41482/CBP Note 247/LHC Project Report 180 (May 20, 1998).

[8] M. A. Furman, "A preliminary assessment of the electron cloud effect for the FNAL main injector upgrade," LBNL-57634/CBP-Note-712/FERMILAB-PUB-05-258-AD, 23 June 2006. A condensed version of this articled, of the same title, is published in New J. Phys. **8** (2006) 279. http://stacks.iop.org/1367-2630/8/279

[9] M. A. Furman, "Studies of e-cloud build up for the FNAL main injector and for the LHC," LBNL-60512/CBP Note-736, June 15, 2006; Proc. 39th ICFA Advanced Beam Dynamics Workshop on High Intensity High Brightness Hadron Beams "HB2006" (Tsukuba, Japan, May 29-June 2nd, 2006), paper TUAX05. http://hb2006.kek.jp/

[10] M. A. Furman, "HINS R&D Collaboration on Electron Cloud Effects: Midyear Progress Report," CBP-Technote-364/FERMILAB-TM-2369-AD, 22 Sept. 2006.

[11] M. A. Furman, "HINS R&D Collaboration on Electron Cloud Effects: Build-Up Simulations at the Electron Detector Location in the MI," CBP Technote-367, Dec. 5, 2006.

[12] M. A. Furman, K. Sonnad and J.-L. Vay, "HINS R&D Collaboration on Electron Cloud Effects: Midyear Report," LBNL-61921/CBP-761/FERMILAB-TM-2370-AD, Nov. 7, 2006.

[13] K. G. Sonnad, M. A. Furman and J.-L. Vay, "A preliminary report on electron cloud effects on beam dynamics for the FNAL main injector upgrade," CBP Technote-369, January 16, 2007.

[14] R. Zwaska, private communication.

[15] R. Kirby, unpublished results, 2006.

DISCLAIMER